

# AIP | The Journal of Chemical Physics

## Study of the electronicvibrational energy transfer in the quenching process of Na(32P) with N2(1Σ+g,v=0). A quantal close coupling calculation

J. CamposMartinez, O. Roncero, S. MiretArtés, P. Villarreal, and G. DelgadoBarrio

Citation: *J. Chem. Phys.* **91**, 155 (1989); doi: 10.1063/1.457494

View online: <http://dx.doi.org/10.1063/1.457494>

View Table of Contents: <http://jcp.aip.org/resource/1/JCPSA6/v91/i1>

Published by the [American Institute of Physics](http://www.aip.org).

### Additional information on J. Chem. Phys.

Journal Homepage: <http://jcp.aip.org/>

Journal Information: [http://jcp.aip.org/about/about\\_the\\_journal](http://jcp.aip.org/about/about_the_journal)

Top downloads: [http://jcp.aip.org/features/most\\_downloaded](http://jcp.aip.org/features/most_downloaded)

Information for Authors: <http://jcp.aip.org/authors>

## ADVERTISEMENT

### Instruments for advanced science

#### Gas Analysis



- dynamic measurement of reaction gas streams
- catalysis and thermal analysis
- molecular beam studies
- dissolved species probes
- fermentation, environmental and ecological studies

#### Surface Science



- UHV TPD
- SIMS
- end point detection in ion beam etch
- elemental imaging - surface mapping

#### Plasma Diagnostics



- plasma source characterization
- etch and deposition process
- reaction kinetic studies
- analysis of neutral and radical species

#### Vacuum Analysis



- partial pressure measurement and control of process gases
- reactive sputter process control
- vacuum diagnostics
- vacuum coating process monitoring

contact Hiden Analytical for further details

**HIDEN**  
ANALYTICAL

[info@hideninc.com](mailto:info@hideninc.com)  
[www.HidenAnalytical.com](http://www.HidenAnalytical.com)

CLICK to view our product catalogue



# Study of the electronic-to-vibrational energy transfer in the quenching process of $\text{Na}^*(3^2P)$ with $\text{N}_2(1^1\Sigma_g^+, v=0)$ . A quantal close coupling calculation<sup>a)</sup>

J. Campos-Martinez, O. Roncero, S. Miret-Artés, P. Villarreal, and G. Delgado-Barrio  
*Instituto de Estructura de la Materia, C/Serrano, 123 28006 Madrid, Spain*

(Received 28 September 1988; accepted 9 March 1989)

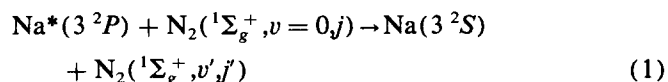
Electronic-to-vibrational energy transfer has been studied by solving numerically the close-coupling equations, in the T-shape configuration, on the two lowest electronic states of the Na- $\text{N}_2$  system. The diabatic potential surfaces were taken from Archirel and Habitz while the interelectronic coupling was modeled by different Gaussian-type functions. Different sets of parameters for the coupling were used in order to study the final vibrational distributions of  $\text{N}_2$ . Finally, partial quenching probabilities are presented and compared with previous theoretical and experimental works.

## I. INTRODUCTION

Intermolecular energy transfer is one of the elementary processes more carefully studied in the nonadiabatic molecular collision. In the low-energy regime, where the kinetic energy associated with nuclear motion is less than  $\sim 20$  eV, an important number of phenomena of this type is found in the astrophysics field, chemical reaction dynamics and gas lasers. In this context, during these last decades, an increasing interest is being addressed to the study of the quenching process of alkali atoms by diatomic molecules or different polyatomic partners. The most refined experimental techniques<sup>1</sup> such as crossed atomic, molecular, and laser beams are being applied in order to improve our understanding of the different mechanisms of energy redistribution. A great deal of experimental data are now available and the interpretation and prediction of these observable is not yet an easy task.

Since the earliest works of Bjerre and Nikitin<sup>2</sup> and Bauer, Fisher, and Gilmore<sup>3</sup> an increasing theoretical effort is being done not only in the obtention of accurate potential energy surfaces (PES's) and reasonable interelectronic couplings<sup>4-8</sup> but also in the application of classical or semiclassical dynamical treatments. In this kind of formalism the surface hopping trajectory (SHT) method<sup>6,8-10</sup> has been one of the most widely used until now. On the other hand, quantal treatments are very infrequent<sup>11-15</sup> and as far as we know no comparison between classical and quantal results has been done.

We are interested here in the collisional quenching



for which a lot of experimental data<sup>15-20</sup> as well as theoretical results from classical calculations<sup>6,8</sup> are now available. This quenching process may be conceptually divided in two steps<sup>21</sup>: (1) Evolution of the system on the upper attractive surface, where vibrational excitation of the diatomic partner may take place, and (2) electronic relaxation of the atom

leading the system to the lower repulsive potential, whose strong anisotropy may induce a high diatomic rotational excitation. Three sets of accurate potential energy surfaces<sup>6-8</sup> for this system are available. Those of Archirel and Habitz<sup>6</sup> show the above features since the excited surface includes terms depending simultaneously on three variables,  $r$  (diatomic bond length),  $\theta$  (relative atom-diatom orientation), and  $R$  (atom-diatom center of mass distance), while in the lower one only mixed  $(R, \theta)$  terms do appear. A similar behavior can be seen by examining the more recent surfaces of Poppe *et al.*<sup>8</sup> As regards to the surfaces of Persico,<sup>7</sup> they were calculated at a fixed  $r$  value, therefore they do not allow accounting for vibrational excitation of the exiting  $\text{N}_2$  molecule.

However, a very important point has been established in that work,<sup>7</sup> that is, the occurrence of the strongest interelectronic couplings in the neighborhood of  $\theta = 0$  and  $\theta = \pi/2$  configurations. Moreover, the region of crossing (or avoided crossing) between both electronic surfaces is located at higher and higher inaccessible energies as we go from the perpendicular to collinear configuration. Thus, it is widely accepted that the atom-diatom orientations around the perpendicular one provide the main contribution to the quenching process.

In this context, a quantal treatment near the  $\theta = \pi/2$  configuration may contribute to shed light about the mechanism of electronic to vibrational energy transfer yielding inversion of vibrational diatomic populations through this collisional quenching. In addition, as it has already been pointed out above, the lower electronic surface of Archirel *et al.* no longer depends at the same time on  $(r, \theta)$  variables and, therefore, vibrational populations of the exiting diatom cannot be modified by its anisotropy. In this way, the final rotational diatomic excitations are being produced by pure translational to rotational energy transfer without change in the exiting vibrational diatomic state.

In this work, we study reaction (1), restricted to a region close to the  $C_{2v}$  symmetry, using a close-coupling formalism within the diabatic frame for a zero total angular momentum. This allows us to estimate final vibrational diatomic distributions together with the efficiency of the quenching process, but the rotational excitation of the  $\text{N}_2$  fragment<sup>6,8</sup> or the quenching cross sections<sup>6,8</sup> are not accounted for in this treatment. The potential surfaces of Ar-

<sup>a)</sup> This work was supported by the C.I.C.Y.T. under Grant No. P80272.

chirel and Habitz,<sup>6</sup> as well as those of Poppe *et al.*,<sup>8</sup> can be used for this purpose. In both cases, the splitting between the two lowest adiabatic surfaces at the avoided crossing seam, determining the interelectronic diabatic coupling, is only a function of  $R$  and  $\theta$ . However, following the ideas of the "bond-stretch attraction model" proposed by Hertel,<sup>1</sup> that coupling is expected to be strongly dependent on  $r$ . Hence, after having taken the diabatic surfaces of Ref. 6 at  $\theta = \pi/2$ , we have used a Gaussian coupling model and examined the role played by its dependence, or not, on the interdiatomic distance. We are aware that the interelectronic diabatic coupling vanishes at exactly  $\theta = \pi/2$ , since the  $^2A_1$  and  $^2B_2$  adiabatic states undergo a crossing in the  $C_{2v}$  configuration. Nevertheless, very close to this configuration,  $\theta = \pi/2 \pm \delta$  ( $\delta > 0$ ), this crossing is avoided. Then, non-zero potential couplings arise showing presumably a quasi-Gaussian look with a maximum at the crossing seam. From this point of view, we assumed that the calculated PES's adequately describe the diabatic surfaces near  $\theta = \pi/2$ ,<sup>12</sup> and our calculations may be considered like a simulation of the collisional quenching within a narrow region around the  $C_{2v}$  symmetry. Therefore, this interelectronic coupling model, in a sense, would account for some angular average, in this  $\theta$  region, through the preexponential parameter. Explicitly, this would imply a factorization of the angular dependence of this coupling, as it is usually assumed in other works<sup>10(a)</sup>.

The paper is organized as follows: In Sec. II, a brief theoretical description of the close-coupling formalism is presented. As will be seen later, this collision requires a high number of closed vibrational channels in the upper electronic state, suggesting an important resonant behavior. Finally, in Sec. III, two different coupling models are considered and the corresponding results are presented and discussed.

## II. THEORY

### A. Close-coupling equations

Assuming a zero total angular momentum and a fixed relative angular orientation, the Hamiltonian for a X + BC triatomic system may be written

$$H = -\frac{\hbar^2}{2\mu} \frac{\partial^2}{\partial R^2} - \frac{\hbar^2}{2m} \frac{\partial^2}{\partial r^2} + H^{\text{el}}(\{q_i\}, R, r), \quad (2)$$

where  $\mu = m_X(m_B + m_C)/(m_X + m_B + m_C)$  and  $m = m_B m_C/(m_B + m_C)$  are reduced masses,  $R$  is the distance between X and the center of mass of BC, and  $r$  is the BC bond length, while  $H^{\text{el}}$  denotes the electronic Hamiltonian depending on the electronic coordinates  $\{q_i\}$  as well as on  $R$  and  $r$ . In the diabatic representation,<sup>22</sup> the set of orthonormal electronic functions  $\xi_{\alpha}(\{q_i\})$  permits us to expand the total wave function as

$$\psi(\{q_i\}, R, r) = \sum_{\alpha} \varphi_{\alpha}(R, r) \xi_{\alpha}(\{q_i\}). \quad (3)$$

By substituting this expression in the usual Schrödinger equation  $H\psi = E\psi$ , premultiplying by  $\xi_{\alpha}^*$ , and integrating over the electronic variables, the following system of coupled equations is reached:

$$\left[ -\frac{\hbar^2}{2\mu} \frac{\partial^2}{\partial R^2} - \frac{\hbar^2}{2m} \frac{\partial^2}{\partial r^2} + V_{\alpha\alpha}(R, r) - E \right] \varphi_{\alpha}(R, r) = - \sum_{\alpha' \neq \alpha} V_{\alpha\alpha'}(R, r) \varphi_{\alpha'}(R, r), \quad (4)$$

where  $V_{\alpha\alpha'}(R, r) = \langle \xi_{\alpha} | H^{\text{el}} | \xi_{\alpha'} \rangle_{\{q_i\}}$ . The diagonal elements  $V_{\alpha\alpha}$  represent effective potential surfaces in the  $\alpha$  electronic state for nuclear motion. At  $R$  long distances, they correlate with the energy of the X atom in a given electronic state plus a precise  $r$ -dependent electronic curve of the diatom BC. On the other hand, the nondiagonal elements,  $V_{\alpha\alpha'}$ ,  $\alpha \neq \alpha'$ , are responsible for electronic transitions. In the particular case under consideration, we assume a two-state electronic problem,  $\alpha = 1, 2$ , involving only the two lowest electronic states in the region around the  $C_{2v}$  symmetry.

By expanding again the diabatic nuclear functions  $\varphi_{\alpha}(R, r)$  in terms of vibrational diatomic eigenfunctions corresponding to the ground electronic state  $\chi_v(r)$ ,

$$\varphi_{\alpha}(R, r) = \sum_v \phi_{\alpha v'}(R) \chi_{v'}(r) \quad (5)$$

and carrying them to the system of Eq. (4), we obtain, after doing a scalar product by  $\chi_v$ , the  $R$ -dependent coupled equations

$$\left[ -\frac{\hbar^2}{2\mu} \frac{d^2}{dR^2} + V_{\alpha v, \alpha v}(R) + \epsilon_v - E \right] \phi_{\alpha v}(R) = - \sum_{(\alpha' v') \neq (\alpha v)} V_{\alpha v, \alpha' v'}(R) \phi_{\alpha' v'}(R), \quad \alpha, \alpha' = 1, 2, \quad (6)$$

where  $\epsilon_v$  is the diatomic eigenvalue corresponding to a vibrational quantum number  $v$  in the ground electronic state while the  $V$  functions are

$$V_{\alpha v, \alpha' v'}(R) = \langle \chi_v(r) | V_{\alpha\alpha'}(R, r) | \chi_{v'}(r) \rangle. \quad (7)$$

The solution of the set of Eq. (6) with the usual boundary conditions, at a given energy  $E$ , provides us the desired partial quenching probabilities

$$P_{\alpha=1, v=0 \rightarrow \alpha'=2, v'}(E) = |S_{1,0 \rightarrow 2, v'}(E)|^2, \quad (8)$$

where  $\alpha = 1$  represents the initial excited electronic state and  $\alpha = 2$  does the final ground electronic state.

Assuming a Boltzmann distribution in initial kinetic energies  $E_{\text{KIN}}^{(\alpha=1, v=0)} = E - \epsilon^{(1)} - \epsilon_0$ ,  $\epsilon^{(1)}$  being the atomic energy in the entrance channel, the mean quenching probabilities at a given temperature  $T$  may be calculated as

$$\langle P_{1,0 \rightarrow 2, v'} \rangle_T = (KT)^{-1} \int_0^{\infty} dE_{\text{KIN}}^{(1,0)} \exp(E_{\text{KIN}}^{(1,0)}/KT) P_{1,0 \rightarrow 2, v'}(E), \quad (9)$$

where  $K$  is the Boltzmann constant. Finally, the total mean quenching probability at  $T$  temperature becomes

$$\bar{P}_0(T) = \sum_{v'} \langle P_{1,0 \rightarrow 2, v'} \rangle_T. \quad (10)$$

## III. RESULTS AND DISCUSSIONS

### A. Potentials and couplings

The potential surfaces used in our calculations have been taken, as it has been said above, from Archirel and

Habitz.<sup>6</sup> They fitted with analytical expressions the points obtained by a modified Hartree–Fock calculation. These expressions for the ground (*g*) state as well as for the excited (*e*) one contain a diatomic part plus an atom–diatom interaction.

In atomic units these potentials for the C<sub>2v</sub> configuration are, representing by  $U_e$  and  $U_g$  the two first PES's  $V_{\alpha\alpha}(R, r)$  in Eq. (4),

$$U_e(r, R) = F(r, R) + f_1(R) + f_3(R) + U_{N_2}(r), \quad (11)$$

$$U_g(r, R) = f_2(R) + f_3(R) + U_{N_2}(r), \quad (12)$$

where

$$F(r, R) = -0.1105 - 1.05e^{-0.93R} - 0.24e^{-0.14(R-3)^2}(r-2.07),$$

$$f_1(R) = -0.006e^{-0.3(R-4.5)^2},$$

$$f_2(R) = -0.1881 + 0.4e^{-0.75R},$$

$$f_3(R) = 111.0e^{-2.14R},$$

and for N<sub>2</sub> we have used a harmonic and anharmonic oscillator with the parameters that appear in Ref. 23.

On the other hand, the evaluation of interelectronic coupling elements and interpolation present some peculiar difficulties and assume a critical importance in the case of avoided crossing.<sup>7</sup> Thus, there is a lack of information about convenient interelectronic couplings that appear in the coupled equations (6). So that, usually, the interelectronic coupling has been modeled by different kind of functions as in quantal treatments mentioned above. In collision ionization processes an exponential form has been used<sup>24</sup> by fitting their parameters to previously available data. However, in a case similar to the one studied here, McGuire *et al.*<sup>12</sup> have employed a Gaussian function for modeling the nonadiabatic electronic coupling in a diabatic representation. In the Na–N<sub>2</sub> case, although we do not have a complete grid of calculated coupling points, Persico<sup>7</sup> has performed an *ab initio* calculation, and also he has calculated the interaction matrix elements between diabatic states. Unfortunately, potentials and couplings were computed at a fixed value of *r* (diatomic bond length) but they are a good guide for understanding both the behavior and shape of the interelectronic couplings in Na–N<sub>2</sub>. Persico found out that the value of the interelectronic coupling increases in going from very large to moderate *R* values, as the local symmetry of the Na atom is more and more perturbed by the presence of N<sub>2</sub>. He explains the inversion of this trend around a given *R* value as prob-

ably due to the increasingly ionic character of the diabatic basis. In fact, when the unpaired electron is localized, respectively, on Na in the  $|\xi_1\rangle$  diabatic state, and on N<sub>2</sub> in  $|\xi_2\rangle$ , the  $\langle\xi_1|H^{\text{el}}|\xi_2\rangle$  interaction should be weak. Then the shape and behavior of the interelectronic coupling could be well represented by a Gaussian function (see Fig. 4 in Persico<sup>7</sup>). Moreover, due to the place where the crossing seam between PES's is located, the wave functions will vanish on the left near the crossing, and therefore an exponential or a Gaussian model for the coupling would lead to similar results.

Thus, we here modeled this coupling by a Gaussian-type function, i.e.,

$$V_{\alpha\alpha'}(r, R) = B \exp[-\beta(R - R_c)^2]. \quad (13)$$

That implies

$$V_{\alpha v, \alpha' v'}(R) = \langle\chi_v(r)|V_{\alpha\alpha'}(r, R)|\chi_{v'}(r)\rangle = \delta_{vv'} B \exp[-\beta(R - R_c)^2]. \quad (14)$$

The preexponential parameter *B* gives an idea of the “strength” of the coupling,  $\beta$  determines its “width”, and *R<sub>c</sub>* is the point where the Gaussian function is centered. The values taken for *B* and  $\beta$  have been reasonably chosen in order to reproduce the experimental data and after different tests, we took the following values *B* = 0.001 a.u. and  $\beta$  = 8 a.u.<sup>−1</sup> Varying the coupling-width parameter in Eq. (13) we can shift slightly the distribution of probabilities and change the magnitude of the distributions of probabilities. The last effect is amplified also varying the *B* parameter but the relative inelastic probabilities are conserved here.

A parameter that must be treated with special attention is *R<sub>c</sub>*. In Table I we present the final partial quenching probabilities at different kinetic energies by using two *R<sub>c</sub>* values. The first one, *R<sub>c</sub>* = 3.437 a.u., is the crossing point of minimum energy in the crossing seam between both ground and excited electronic surfaces (similar to the McGuire and Bellum choice<sup>12</sup>). It can be seen that the inversion of population obtained depends on the kinetic energy range studied, mainly for the case where *R<sub>c</sub>* = 3.437 a.u. This point is situated far on the left from the return classic points at these energies. Therefore, the coupling between the continuum wave functions is smaller than for the case where the Gaussian function is centered at *R<sub>c</sub>* = 4.12 a.u. Furthermore, this point is near to crossing between the entry *v* = 0 channel and the exit *v'* = 2 channel while *R<sub>c</sub>* = 3.437 a.u. is the crossing point between the *v* = 0 and *v'* = 0 channel. Thus, the shape of these vibrational distributions can be monitored by using

TABLE I. Transition probabilities from the *v* = 0 channel of the excited electronic state to the *v'* = *n* channel of the ground electronic state, as a function of the initial relative kinetic energy, *E<sub>k</sub>* (in cm<sup>−1</sup>). The parameters used in the calculations were *B* = 0.001 a.u. and  $\beta$  = 8 a.u.<sup>−1</sup> for the coupling of Eq. (14). The superindex denotes the crossing point in a.u.

<i>E<sub>k</sub></i>	(3.437) <i>P</i> <sub>0→0'</sub>	(3.437) <i>P</i> <sub>0→1'</sub>	(3.437) <i>P</i> <sub>0→2'</sub>	(4.12) <i>P</i> <sub>0→0'</sub>	(4.12) <i>P</i> <sub>0→1'</sub>	(4.12) <i>P</i> <sub>0→2'</sub>	(4.12) <i>P</i> <sub>0→3'</sub>
110	1.752 (−5)	2.355 (−4)	1.072 (−6)	3.815 (−4)	1.316 (−2)	5.526 (−2)	4.956 (−3)
210	1.076 (−4)	1.204 (−4)	2.348 (−6)	1.539 (−4)	1.806 (−2)	5.162 (−2)	4.661 (−3)
310	3.735 (−4)	6.510 (−5)	5.333 (−6)	3.010 (−5)	2.422 (−2)	4.479 (−2)	5.113 (−3)
410	6.139 (−4)	1.278 (−5)	7.543 (−6)	2.620 (−6)	2.978 (−2)	4.042 (−2)	4.802 (−3)

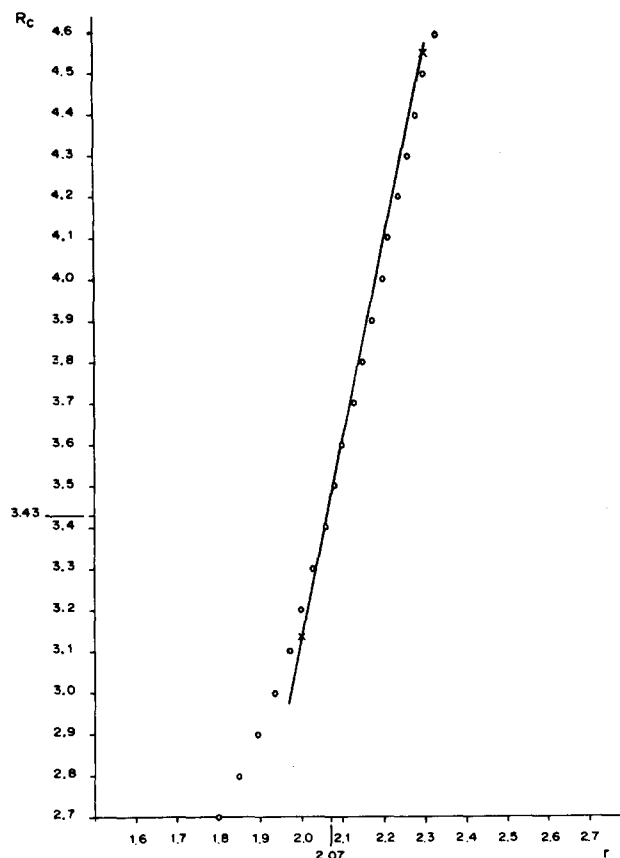


FIG. 1. A fitting of the crossing seam  $R_c(r)$  to a straight line around the equilibrium position of the  $\text{N}_2$  oscillator ( $r = 2.07$  a.u.). All magnitudes are in atomic units.

TABLE II. Values for  $R_c(r)$  at several angles near  $\theta = \pi/2$ . The value  $r = 2.07$  is fixed to the equilibrium position of the  $\text{N}_2$  molecule.

$\theta$ (°)	85	86	87	88	89	90
$R_c(r)$	1.399	1.899	2.381	2.860	3.265	3.437

simple interelectronic coupling centered in some adequate point.

With all this in mind, and taking into account the “bond stretch model” proposed by Hertel<sup>1</sup> for the electronic energy transfer, we used as coupling the following expression:

$$V_{av,\alpha'v'}(R) = B \langle \chi_v(r) | e^{-\beta[R - R_c(r)]^2} | \chi_{v'}(r) \rangle, \quad (15)$$

where, in this formula,  $R_c(r)$  is the crossing seam of the two electronic surfaces involved in the process. So we introduce the dependence on  $r$  in the interelectronic coupling, because the vibration of  $\text{N}_2$  is important for it, as was pointed out by several authors. Therefore, this coupling contains information arising from the PES's. Thus the proper distribution is produced by the PES's themselves.

In Fig. 1 we plot  $R_c(r)$  vs  $r$ . This curve can be fitted by a straight line, around the equilibrium position of the  $\text{N}_2$  oscillator. This fitting is feasible not only for the  $C_{2v}$  configuration but also for other angles between  $r$  and  $R$ . In Table II we present for different angles and  $r = 2.07$  a.u., the corresponding  $R_c(r)$  values. It is interesting to note that  $R_c(r)$  decreases rapidly as  $\theta$  goes away from the  $C_{2v}$  configuration and in consequence the crossing between both lower PES's is located at higher energies. This fact, as was said above, sup-

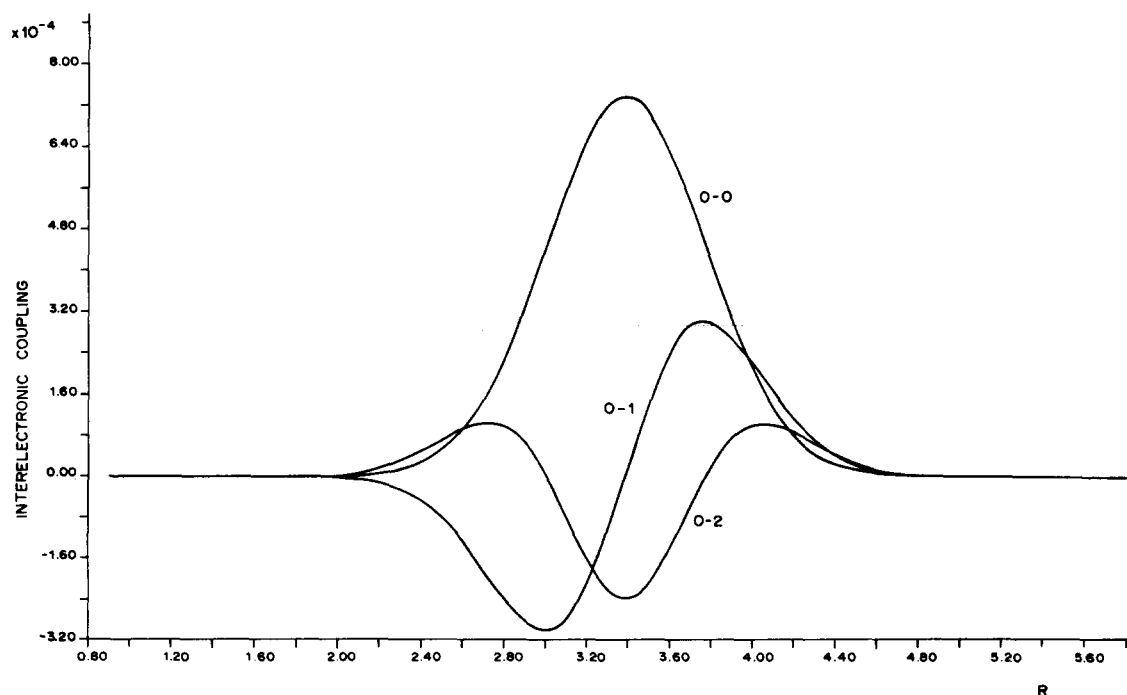


FIG. 2. Interelectronic couplings represented by Eq. (15). All magnitudes are in atomic units.

TABLE III. Transition probabilities from the  $v = 0$  channel of the excited electronic state to the  $v' = n$  channel of the ground electronic state as well as elastic probabilities of the quenching process as a function of the initial relative kinetic energy,  $E_k$  (in cm<sup>-1</sup>). Again, the parameters used are  $B = 0.001$  a.u. and  $\beta = 8$  a.u.<sup>-1</sup> for the coupling of Eq. (15). N<sub>2</sub> is a harmonic oscillator.

$E_k$	$P_{0 \rightarrow 0'}$	$P_{0 \rightarrow 1'}$	$P_{0 \rightarrow 2'}$	$P_{0 \rightarrow 3'}$	$P_{0 \rightarrow 4'}$	Elastic probability
10	0.335 ( - 3)	0.643 ( - 2)	0.556 ( - 1)	0.158 ( - 1)	0.163 ( - 3)	0.9212
210	0.177 ( - 2)	0.144 ( - 1)	0.494 ( - 1)	0.156 ( - 1)	0.219 ( - 3)	0.9186
410	0.416 ( - 2)	0.240 ( - 1)	0.399 ( - 1)	0.128 ( - 1)	0.438 ( - 3)	0.9187
610	0.727 ( - 2)	0.341 ( - 1)	0.294 ( - 1)	0.960 ( - 2)	0.727 ( - 3)	0.9189
810	0.109 ( - 1)	0.435 ( - 1)	0.161 ( - 1)	0.518 ( - 2)	0.149 ( - 2)	0.9217
1010	0.168 ( - 1)	0.493 ( - 1)	0.124 ( - 1)	0.458 ( - 2)	0.973 ( - 3)	0.9159
1210	0.189 ( - 1)	0.578 ( - 1)	0.535 ( - 2)	0.207 ( - 2)	0.121 ( - 2)	0.9148
1410	0.221 ( - 1)	0.620 ( - 1)	0.132 ( - 2)	0.658 ( - 3)	0.128 ( - 2)	0.9127
1610	0.261 ( - 1)	0.632 ( - 1)	0.604 ( - 4)	0.311 ( - 3)	0.124 ( - 2)	0.9091
1810	0.277 ( - 1)	0.625 ( - 1)	0.140 ( - 2)	0.112 ( - 3)	0.107 ( - 2)	0.9073

port strongly our idea of studying the quenching around the T-shape configuration, because for the other angles the quenching probabilities are negligible. In Fig. 2 we plot some averaged couplings with Eq. (15), they look like those calculated in Ref. 25. This coupling will be employed in the next section and it is the coupling model proposed in this work for studying the quenching process.

## B. Final vibrational distributions

In Table III, we present the quenching probabilities  $P_{0 \rightarrow n'}$ , where  $v = 0$  and  $v' = n$  are the entry and exit vibrational channels, together with the elastic probabilities at different kinetic energies,  $E_k$  (cm<sup>-1</sup>), and for  $B = 0.001$  a.u. and  $\beta = 8$  a.u.<sup>-1</sup>. We can observe that the inversion of the final vibrational population depends on the kinetic energy. This fact is also seen when we use an anharmonic potential for describing the diatomic molecule as is shown in Table IV.

The maxima obtained for the population were for  $v' = 2$  at low kinetic energies and  $v' = 1$  for higher ones, in the harmonic case, and remain  $v' = 2$  in the same range for the anharmonic description. The only difference between both calculations is the potential describing the diatomic (harmonic or anharmonic). This potential influences in the separation among vibrational channels and also in the coupling. With an anharmonic potential the vibrational channels are

more and more close while this separation is kept constant in the harmonic case. With respect to the couplings, their values are similar but in the anharmonic case all vibrational channels are connected by means of the  $(r - 2.07)$  term that appears in Eq. (11) (upper electronic state) while only consecutive channels are coupled in a harmonic description.

In Table V we compare some theoretical results for final vibrational population at  $E_k = 0.17$  eV with our results. The two first columns have been obtained with a SHT method but using different dynamical models, PES's, and couplings. Only the second column represents a three-dimensional calculation and the PES's for the perpendicular configuration are the same than those used in this work. A peak in  $v' = 2$  is obtained for all the four distributions but the population in each exit channel is different. However, a good qualitative agreement is found when we compare the three-dimensional classical calculation with the T-shape quantal model. This result is not surprising because, after quenching, the coupling term appearing in the ground state among  $R$ ,  $r$ ,  $\theta$  is very small. Thus, the final vibrational population is not modified on this state. Moreover, the quenching process, as it was said above, only is effective for angles around  $\pi/2$  [i.e., if  $R_c(r)$  is not very small]. In general, theoretical calculations show similar results, with a maximum for the  $v' = 2$  vibrational level [see, for instance, Refs. 1 and 10(a) for a

TABLE IV. Transition probabilities from the  $v = 0$  channel of the excited electronic state to the  $v' = n$  channel of the ground electronic state together with elastic probabilities.  $E_k$  is the relative kinetic energy in cm<sup>-1</sup>, and  $B, \beta$  are the same as used in Table III. Here, N<sub>2</sub> is considered as an anharmonic oscillator.

$E_k$	$P_{0 \rightarrow 0'}$	$P_{0 \rightarrow 1'}$	$P_{0 \rightarrow 2'}$	$P_{0 \rightarrow 3'}$	$P_{0 \rightarrow 4'}$	Elastic probability
10	0.385 ( - 2)	0.297 ( - 1)	0.315 ( - 1)	0.289 ( - 1)	0.348 ( - 4)	0.906
210	0.498 ( - 2)	0.245 ( - 1)	0.403 ( - 1)	0.333 ( - 1)	0.584 ( - 4)	0.897
410	0.520 ( - 2)	0.206 ( - 1)	0.476 ( - 1)	0.340 ( - 1)	0.425 ( - 3)	0.892
610	0.583 ( - 2)	0.156 ( - 1)	0.522 ( - 1)	0.340 ( - 1)	0.987 ( - 3)	0.891
810	0.615 ( - 2)	0.115 ( - 1)	0.403 ( - 1)	0.334 ( - 1)	0.271 ( - 2)	0.901
1010	0.622 ( - 2)	0.681 ( - 2)	0.538 ( - 1)	0.287 ( - 1)	0.286 ( - 2)	0.901
1210	0.465 ( - 2)	0.227 ( - 2)	0.460 ( - 1)	0.240 ( - 1)	0.196 ( - 2)	0.921
1410	0.467 ( - 2)	0.916 ( - 3)	0.443 ( - 1)	0.181 ( - 1)	0.397 ( - 2)	0.927
1610	0.510 ( - 2)	0.985 ( - 4)	0.394 ( - 1)	0.151 ( - 1)	0.593 ( - 2)	0.934
1810	0.435 ( - 2)	0.195 ( - 3)	0.314 ( - 1)	0.111 ( - 1)	0.537 ( - 2)	0.947

TABLE V. Comparison of experimental and theoretical vibrational populations for the process:  $\text{Na}^* + \text{N}_2(v=0) \rightarrow \text{Na} + \text{N}_2(v')$ .  $P_n$ 's are the relative quenching probabilities,  $P_{0 \rightarrow n}$ .

	Ref. 10(a)	Ref. 6(b)	This work	
			Harmonic	Anharmonic
$P_0$	0.085	0.030	0.104	0.049
$P_1$	0.185	0.100	0.380	0.165
$P_2$	0.221	0.387	0.385	0.461
$P_3$	0.196	0.252	0.118	0.302
$P_4$	0.143	0.156	0.009	0.014
$P_5$	0.091	0.061	0.001	0.004
$P_6$	0.052	0.009	0.5(−3)	0.002
$P_7$	0.026	0.004	0.5(−3)	1.0(−4)

comparison and discussion with earlier theoretical works]. Experimentally, however, the final vibrational populations are peaked at  $v' = 3,4$  depending on experiment.<sup>16,17</sup> In the work of Gislason *et al.*<sup>10(a)</sup> is commented that previous semi-classical approaches did not treat the vibrational motion properly and, consequently, the theoretical distributions were not in satisfactory agreement with experiment. They recognized that for obtaining final vibrational populations, it is necessary to use a quantum mechanical theory for describing the vibrational motion. Then, they considered this motion in a quantum way, but no *ab initio* PES's were used and also a vibrational decoupling from the translational motion was assumed. With the "bond-stretch model" in mind, this decoupling seems to be unappropriated, although the use of the new *ab initio* PES's should probably allow the improvement of their results. On the other hand, in the work of Archirel *et al.*,<sup>6</sup> *ab initio* PES's were used but again the vibrational motion was treated classically, nevertheless, no further dynamical approximations were made. This is the main advantage of using classical mechanics for the quenching process as compared with three-dimensional quantal calculations. These are feasible but they are very expensive and, therefore, additional assumptions in order to make the calculations tractable are required. In spite of this, quantal approaches (such as the work presented here), allow a great physical insight into the mechanism of the quenching process.

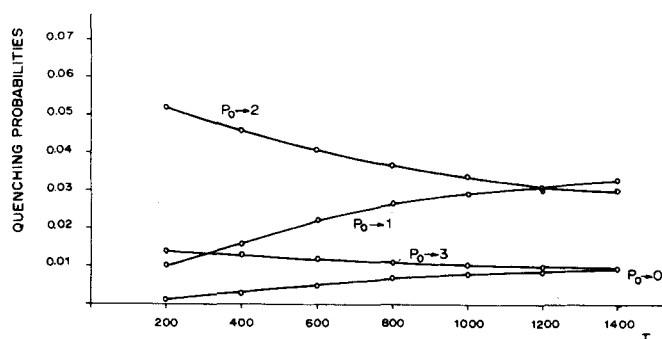


FIG. 3. Behavior of the quenching probabilities as a function of the temperature (K), when N<sub>2</sub> is described as a harmonic oscillator.

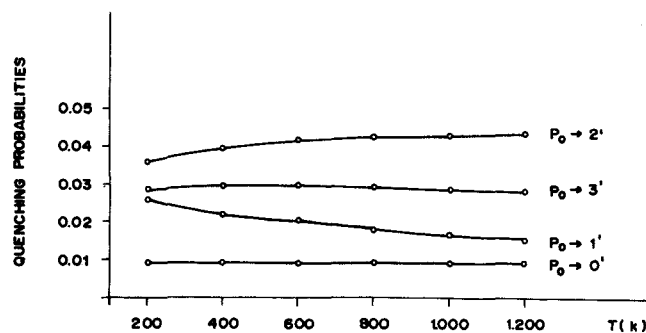


FIG. 4. Behavior of the quenching probabilities as a function of the temperature (K), when an anharmonic oscillator is taken for describing the N<sub>2</sub> molecule.

In Fig. 3 we present the averaged transition probabilities using a Maxwell-Boltzmann distribution with a harmonic potential for N<sub>2</sub> and in Fig. 4 the same for the anharmonic case. In the anharmonic case, the inversion of population remains when the temperature is going up, while in the harmonic case, it decreases with temperature. An experimental study would be very interesting in order to analyze the evolution of these vibrational populations with kinetic energy (or temperature). The stability of these distributions would indicate, if experimentally found, the importance of anharmonicity in the process.

At 1200 K, the energy transferred to the vibrational motion of N<sub>2</sub>, when the Na has been quenched, is about 20% in harmonic and the 26% in the anharmonic oscillator. The experimental results of Silver *et al.*<sup>16</sup> give between 30% and 40% while Reiland *et al.*<sup>17</sup> have obtained about 50%. The discrepancy between the experimental and theoretical results is due to the different final vibrational populations. The experimental ones are peaked at one or two vibrational quantum numbers greater than that found in the theoretical studies. However, following Kompa *et al.*<sup>26</sup> only a limited knowledge of these distributions can be obtained in this kind of experiment, but direct measurements of the population distribution of the quencher are not easy. A useful technique

TABLE VI. Partial quenching probabilities at some different relative kinetic energies ( $E_k$ , in  $\text{cm}^{-1}$ ). On the left side, all channels are open while on the right one, closed channels have been used until numerical convergence was reached, N<sub>2</sub> being a harmonic oscillator.

$E_k$	All channels open			
	$P_{0 \rightarrow 0'}$	$P_{0 \rightarrow 1'}$	$P_{0 \rightarrow 2'}$	$P_{0 \rightarrow 3'}$
110	2.819 (−4)	5.404 (−3)	2.559 (−3)	1.870 (−4)
1010	1.585 (−3)	1.437 (−2)	4.840 (−4)	1.139 (−4)
$E_k$	Ten closed channels			
	$P_{0 \rightarrow 0'}$	$P_{0 \rightarrow 1'}$	$P_{0 \rightarrow 2'}$	$P_{0 \rightarrow 3'}$
	8.871 (−4)	1.039 (−2)	5.300 (−2)	1.638 (−2)
	1.677 (−2)	4.931 (−2)	1.243 (−2)	4.582 (−3)

seems to be the coherent anti-Stokes–Raman spectroscopy (CARS) to measure directly the internal energy distribution of the diatomic.

All the calculations were performed with nine channels in the ground electronic state and ten in the first excited state. The number of closed channels necessary for the numerical convergency was ten (nine in the excited state). In Table VI, we present at some kinetic energies the different probabilities in the exit channels obtained with and without closed channels in the harmonic case. As it can be seen, the total quenching probability is greater by a factor  $\sim 5$  when we introduce into the calculation the closed channels. Moreover, the vibrational excitation is greater with than without closed channels. The importance of the closed channels was already pointed out by Hertel<sup>1</sup> and this fact shows that the quenching process is not a direct one. The resonances could play an important role. For the anharmonic case, the results obtained in the same way are very similar to those presented in this table.

In order to test the possible resonances that exist in the quenching process, it would be important to study the presence of metastable levels. In this sense, the application of a diabatic (D) and a diabatic–configuration interaction (D–CI)<sup>27</sup> model would be useful in the calculation of the quasi-bound levels and the corresponding lifetime. Works in this direction are now in progress.<sup>28</sup>

#### IV. CONCLUSIONS

We have carried out the first quantal close-coupling calculation of the Na–N<sub>2</sub> system. Although restricted to  $C_{2v}$  configuration, we have seen that only in (or around)  $\theta = \pi/2$ , quenching probabilities are not negligible. In any case, the stretching of diatomic bond, included in our coupling model, is important in order to explain this process. The main features of this system can be studied with the coupling model proposed here, together with the *ab initio* PES's.

<sup>1</sup>(a) I. V. Hertel, in *Dynamics of the Excited State*, edited by K. Lawley (Wiley New York, 1982), p. 475; (b) W. H. Breckenridge and H. Umemoto, *ibid.*, p. 325; (c) A. W. Kleyn, J. Los, and E. A. Gislason, *Phys. Rep.* **90**, 1 (1982).

- <sup>2</sup>A. Bjerre and E. E. Nikitin, *Chem. Phys. Lett.* **1**, 179 (1967).  
<sup>3</sup>E. Bauer, E. R. Fisher, and F. R. Gilmore, *J. Chem. Phys.* **51**, 4173 (1969).  
<sup>4</sup>(a) P. Botschwina, W. Meyer, I. V. Hertel, and W. Reiland, *J. Chem. Phys.* **75**, 5438 (1981); (b) W. Reiland, H. -U. Tittes, I. V. Hertel, V. Bonačić-Koutecký, and M. Persico, *ibid.* **77**, 1908 (1982).  
<sup>5</sup>(a) D. G. Truhlar, J. W. Duff, N. C. Blais, J. C. Tully, and B. C. Garrett, *J. Chem. Phys.* **77**, 764 (1982); (b) N. C. Blais, D. G. Truhlar, and B. C. Garrett, *ibid.* **78**, 2956 (1983).  
<sup>6</sup>(a) P. Habitz, *Chem. Phys.* **54**, 131 (1980). (b) P. Archirel and P. Habitz, *ibid.* **78**, 213 (1983).  
<sup>7</sup>M. Persico, in *Spectral Line Shapes* (De Gruyter, Berlin, 1985), Vol. III.  
<sup>8</sup>D. Poppe, D. Papierowska-Kaminski, and V. Bonačić-Koutecký, *J. Chem. Phys.* **86**, 822 (1987).  
<sup>9</sup>J. C. Tully, in *Dynamics of Molecular Collisions*, Part B, edited by W. H. Miller (Plenum, New York, 1976), p. 217.  
<sup>10</sup>(a) E. A. Gislason, A. W. Kleyn, and J. Los, *Chem. Phys.* **59**, 91 (1981); (b) N. C. Blais and D. G. Truhlar, *J. Chem. Phys.* **79**, 1334 (1983).  
<sup>11</sup>G. Delgado-Barrio and J. A. Beswick, *Chem. Phys. Lett.* **48**, 358 (1977).  
<sup>12</sup>P. McGuire and J. C. Bellum, *J. Chem. Phys.* **71**, 1975 (1979).  
<sup>13</sup>C. H. Becker and R. P. Saxon, *J. Chem. Phys.* **75**, 4899 (1981).  
<sup>14</sup>J. Campos-Martinez, O. Roncero, S. Miret-Artés, P. Villarreal, and G. Delgado-Barrio, *Atomic and Molecular Processes with Short Intense Laser Pulses*, NATO ASI Series, edited by A. D. Bandrauk (Plenum, New York, 1987).  
<sup>15</sup>J. R. Barker and R. E. Weston, Jr., *J. Chem. Phys.* **65**, 1427 (1976).  
<sup>16</sup>J. A. Silver, N. C. Blais, and G. H. Kwei, *J. Chem. Phys.* **71**, 3412 (1979).  
<sup>17</sup>W. Reiland, C. P. Schulz, H. -U. Tittes, and I. V. Hertel, *Chem. Phys. Lett.* **91**, 329 (1982).  
<sup>18</sup>I. Tanarro, F. Arquerros, and J. Campos, *J. Chem. Phys.* **77**, 1826 (1982).  
<sup>19</sup>W. Kamke, B. Kamke, I. V. Hertel, and A. Gallagher, *J. Chem. Phys.* **80**, 4879 (1984).  
<sup>20</sup>G. Jamieson, W. Reiland, C. P. Schulz, H. -U. Tittes, and I. V. Hertel, *J. Chem. Phys.* **81**, 5805 (1984).  
<sup>21</sup>D. Poppe, *Chem. Phys.* **111**, 17 (1987).  
<sup>22</sup>M. S. Child, in *Atom–Molecule Collision Theory*, edited by R. B. Bernstein (Plenum, New York, 1979), p. 427.  
<sup>23</sup>G. Herzberg, *Spectra of Diatomic Molecules* (Van Nostrand Reinhold, New York, 1979).  
<sup>24</sup>(a) R. Grice and D. R. Herschbach, *Mol. Phys.* **27**, 159 (1974); (b) M. B. Faist, B. R. Johnson, and R. D. Levine, *Chem. Phys. Lett.* **32**, 1 (1975); (c) M. B. Faist, and R. D. Levine, *J. Chem. Phys.* **64**, 2953 (1976); (d) A. W. Kleyn, M. M. Hubers, and J. Los, *Chem. Phys.* **34**, 55 (1978); (e) A. W. Kleyn, V. N. Khromov, and J. Los, *ibid.* **52**, 65 (1980).  
<sup>25</sup>C. Galloy and J. C. Lorquet, *J. Chem. Phys.* **67**, 4672 (1977).  
<sup>26</sup>P. Hering, S. L. Cunha, and K. L. Kompa in *Methods Laser Spectroscopy*, edited by Y. Prior, Reuven A. Ben, and M. Rosenbenh (Plenum, New York, 1985).  
<sup>27</sup>P. Villarreal, G. Delgado-Barrio, O. Roncero, F. A. Gianturco, and A. Palma, *Phys. Rev. A* **336**, 617 (1987).  
<sup>28</sup>J. Campos-Martinez, P. Villarreal, G. Delgado-Barrio, and S. Miret-Artés, *Int. J. Quantum Chem.* (in press).